

$^{174}\text{Yb}^+ - ^{113}\text{Cd}^+$ sympathetic-cooling bi-species Coulomb crystal applied to microwave frequency standard.

Y Zheng,^{1,2, a)} H. R. Qin,^{1,2, a)} S. N. Miao,¹ N. C. Xin,¹ Y. T. Chen,¹ J. Z. Han,¹ J. W. Zhang,^{1, b)} and L. J. Wang^{1,2}

¹⁾State Key Laboratory of Precision Measurement Technology and Instruments, Key Laboratory of Photon Measurement and Control Technology of Ministry of Education, Department of Precision Instrument, Tsinghua University, Beijing 100084, China

²⁾Department of Physics, Tsinghua University, Beijing 100084, China

We reported the realization of a $^{174}\text{Yb}^+ - ^{113}\text{Cd}^+$ bi-species Coulomb crystal comprising $^{174}\text{Yb}^+$ ions as coolant and verified its potential for application as a $^{113}\text{Cd}^+$ microwave frequency standard employing sympathetic cooling. The two species of massive ions stably trapped in a Paul trap make up this large two-component crystal. The $^{113}\text{Cd}^+$ ions are trapped in the center, which reduces considerably RF heating and excess micromotion to which the $^{113}\text{Cd}^+$ ions are subjected. Under this scheme, the uncertainty due to the second-order Doppler effect is reduced to 5×10^{-16} , which represents an order of magnitude improvement over sympathetic cooled $^{40}\text{Ca}^+ - ^{113}\text{Cd}^+$ crystal. The uncertainty from the second-order Zeeman effect, which contributes the largest uncertainty to the microwave-ion frequency standard, is reduced to 4×10^{-16} . The relevant AC Stark shift uncertainty is estimated to be 4×10^{-19} . These results indicate using $^{174}\text{Yb}^+$ as coolant ions for $^{113}\text{Cd}^+$ is far superior and confirm the feasibility of a sympathetic-cooled cadmium-ion microwave clock system employing a $^{174}\text{Yb}^+ - ^{113}\text{Cd}^+$ two-component crystal.

Atomic clocks have been playing an important role in both practical applications¹ and basic physics research²⁻⁴. Microwave clocks are widely used in satellite navigation^{5,6}, deep space exploration^{7,8}, time synchronization⁹ and timekeeping^{10,11} because of their simple structure and high transportability. At present, a lot of important progress has been made with microwave ion clocks that employ trapped $^{199}\text{Hg}^+$ ^{8,11,12}, $^{171}\text{Yb}^+$ ^{13,14}, $^{113}\text{Cd}^+$ ¹⁵⁻¹⁷ ions.

In past work, we have realized highly stable and accurate microwave ion clocks based on laser-cooled $^{113}\text{Cd}^+$ ions¹⁵⁻¹⁷. However, laser-cooled ion microwave clocks require a separate cooling process, which results in dead time. The dead time restricts the Dick effect limit, thereby preventing improvements in short-term stability. In addition, the ions are not cooled during microwave interrogation. The temperature increase leads to second-order Doppler shift (SODS) and limits the linewidth and signal-to-noise ratio (SNR) of the clock signal. To solve the above problems, we applied the sympathetic cooling technique to $^{113}\text{Cd}^+$ ion microwave clocks¹⁸⁻²⁰.

The first ion microwave clock employing sympathetic cooling was built by the Bollinger group at NBS in 1991, which used $^{24}\text{Mg}^+$ as coolant ions to sympathetically cool $^9\text{Be}^+$ ion in a Penning trap. Their experiment showed the potential of sympathetic cooling applied to ion microwave clock. Since 2019, our group has been devoted to research the cadmium ion microwave frequency standard based on sympathetic cooling. We first used $^{24}\text{Mg}^+$ as coolant²¹. However, the cooling laser of $^{24}\text{Mg}^+$ ions is not easy to obtain and the reaction between Mg^+ and H_2 in the background gas reduces cooling efficiency. We further chose $^{40}\text{Ca}^+$ to sympathetically cool $^{113}\text{Cd}^+$ ^{20,22}. In 2022, we realized a high-performance $^{113}\text{Cd}^+$ ion microwave frequency standard using this scheme, which was the first sympathetically-cooled

ion microwave clock in a Paul trap. $^{113}\text{Cd}^+$ ions were sympathetically cooled with laser-cooled $^{40}\text{Ca}^+$. Its short-term frequency stability reached $3.48 \times 10^{-13}/\sqrt{\tau}$ with frequency uncertainty of 1.5×10^{-14} , which are both better than directly laser-cooled $^{113}\text{Cd}^+$ microwave frequency standard¹⁸.

Although $^{113}\text{Cd}^+$ microwave clock sympathetically cooled with $^{40}\text{Ca}^+$ performed well, several limitations remained. First, the mass difference between the two species of ions is large, making the ion separation ratio relatively large, thereby limiting the efficiency of sympathetic cooling. Second, the mass of $^{40}\text{Ca}^+$ is smaller than $^{113}\text{Cd}^+$; therefore, the latter ions are in the outer layer of the ion crystal surrounding the $^{40}\text{Ca}^+$ ions. Being farther from the trap central axis also results in large RF heating. Moreover, the distance of $^{113}\text{Cd}^+$ ions from the trap center leads to excess micro-motion²³ and second-order Doppler effect²⁴, that again severely limit improvements in frequency accuracy and stability.

A scheme that uses $^{174}\text{Yb}^+$ to sympathetically cool $^{113}\text{Cd}^+$ was incorporated into the microwave frequency standard²⁵ to improve performance. While seldom studied, we demonstrated the viability of $^{174}\text{Yb}^+$ sympathetically-cooling $^{113}\text{Cd}^+$ microwave frequency standard system and realized a large number of sympathetically cooled $^{113}\text{Cd}^+$ with laser-cooled $^{174}\text{Yb}^+$. At present, the frequency accuracy of the ion microwave clock is mainly restricted by the second-order Doppler frequency shift (SODS) and the second-order Zeeman frequency shift (SOZS). Under this scheme, the $^{113}\text{Cd}^+$ ion temperature is as low as 10²mK and the excess micro-motion is greatly suppressed. The uncertainty associated with the SODS is reduced to 5×10^{-16} , which is advanced by an order of magnitude compared with that of $^{40}\text{Ca}^+ - ^{113}\text{Cd}^+$ sympathetic cooling. The uncertainty related to SOZS is reduced to 4×10^{-16} . Our research shows that sympathetic-cooled mixed-species Coulomb crystal of $^{174}\text{Yb}^+ - ^{113}\text{Cd}^+$ is an effective experimental method that improves the performance of the $^{113}\text{Cd}^+$ ion microwave frequency standard.

^{a)}These authors contributed equally.

^{b)}Electronic mail: zhangjw@tsinghua.edu.cn

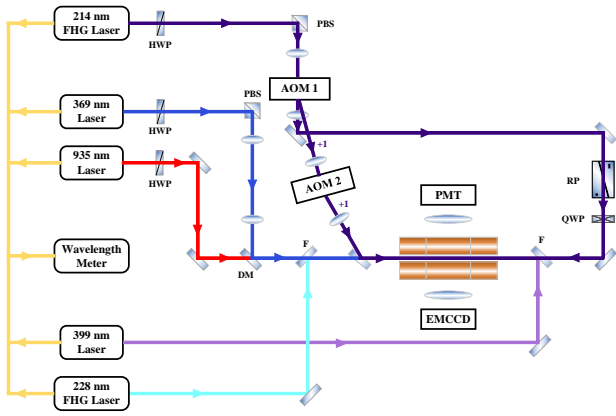


FIG. 1. Schematic diagram of the entire optical system designed. HWP: half-wave plate; PBS: polarization beam splitter; RP: Rochon polarizer; QWP, quarter-wave plate; DM: dichromatic mirror; F: mirror installed on flipper; AOM: acousto-optic modulator.

The ion trap we used has been described in more detail in our previous work¹⁷. The ground state hyperfine splitting frequency of $^{113}\text{Cd}^+$ is 15.2 GHz, ranking second only to $^{199}\text{Hg}^+$ among all working energy levels of atomic microwave clocks. Because the hyperfine splitting frequency of the $^2P_{3/2}$ energy level is only 800 MHz, pumping and detection can be realized by a single laser with acousto-optic modulators. Therefore, the $^{113}\text{Cd}^+$ frequency standard has great potential for high performance and miniaturization. The natural abundance of ^{174}Yb is 31.83%, which is the highest among the seven stable Yb isotopes. Moreover, the cooling laser $^{174}\text{Yb}^+$ requires is easily available. Compared with $^{40}\text{Ca}^+$, $^{174}\text{Yb}^+$ is not only closer in mass but also heavier than $^{113}\text{Cd}^+$. These characteristics indicate that $^{174}\text{Yb}^+$ is well suited as a coolant ion for $^{113}\text{Cd}^+$.

The entire optical system we designed (Fig. 1), incorporates the $^{113}\text{Cd}^+$ component of a previous design¹⁸. The 399 nm laser beam is used to transition ^{174}Yb atom from the ground state $6s^2\ ^1S_0$ to the first excited state $6s6p\ ^1P_1$. Because there is an isotopic shift of approximately 500 MHz between ^{174}Yb and other isotopes²⁶, this photoionization selectively ionizes the ^{174}Yb atoms. For Doppler cooling and repumping of the $^{174}\text{Yb}^+$, the 369 nm laser beam ($6s^2\ ^1S_0 \rightarrow 6p^2\ ^1P_{1/2}$) is combined with the 935 nm laser beam ($^2D_{3/2} \rightarrow ^3[3/2]_{1/2}$) by the dichroic mirror. Photoionization is enabled by turning on the cooling laser with the wavelength of 369 nm while opening the laser with the wavelength of 399 nm to excite the ^{174}Yb atoms.

In the $^{174}\text{Yb}^+$ - $^{113}\text{Cd}^+$ sympathetic cooling stage, we loaded and cooled the $^{174}\text{Yb}^+$ ions to form the crystal first and subsequently loaded the $^{113}\text{Cd}^+$ ions. Then $^{174}\text{Yb}^+$ were heated. We repeated the adjustments to the amplitude of RF voltage and scanned the frequency of the cooling laser (369 nm). The detection by the photomultiplier tube (PMT) of a variation in the fluorescence signal of $^{113}\text{Cd}^+$ indicates the two species of ions have formed a two-component Coulomb crystal.

A typical image captured by the electron-multiplying

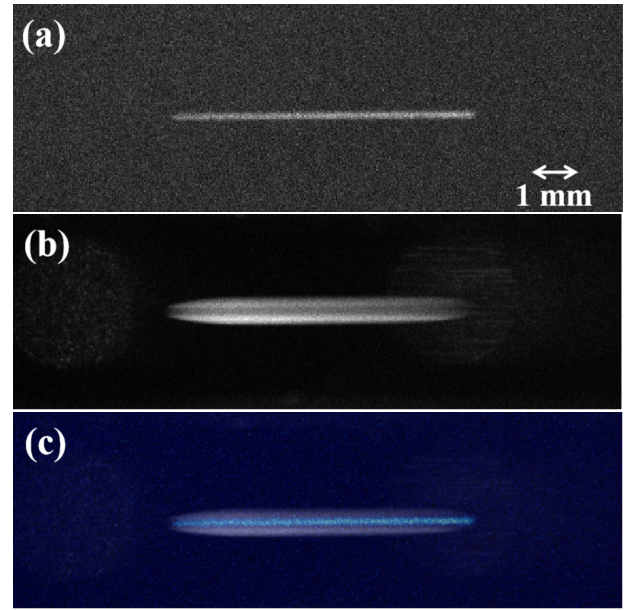


FIG. 2. Typical image of $^{174}\text{Yb}^+$ - $^{113}\text{Cd}^+$ two-component ion crystal with $U_{RF} = 241\text{V}$. (a) Image of $^{113}\text{Cd}^+$ under 214.5 nm wavelength filter. (b) Image of $^{174}\text{Yb}^+$ under 397 nm wavelength filter. (c) Image combined of two images taken by EMCCD under different wavelength filters.

charge-coupled device (EMCCD) of the two-component ion crystal (Fig. 2) depicts a hollow structure of $^{174}\text{Yb}^+$ ions and an ellipsoid of $^{113}\text{Cd}^+$ ions located in the center, which is in line with our expectation in using $^{174}\text{Yb}^+$ as a coolant. To estimate the number of ions, we need to determine the separation ratio and density of the two species of ions. The separation ratio is calculated using²⁷⁻³⁰:

$$\frac{r_{\text{Yb}^+}}{r_{\text{Cd}^+}} = \sqrt{\frac{M_{\text{Yb}^+}}{M_{\text{Cd}^+}}}, \quad (1)$$

where r_{Yb^+} denotes the inner radius of the $^{174}\text{Yb}^+$ crystal shell, r_{Cd^+} the outer radius of the $^{113}\text{Cd}^+$ crystal. We experimentally measured the separation ratio by analyzing the EMCCD images. The result is $r_{\text{Yb}^+}/r_{\text{Cd}^+} = 1.25(3)$, which agrees with the theoretical value of 1.24. Using the zero-temperature charged-liquid model^{28,30}, the ion density is estimated to be:

$$n = \frac{\epsilon_0 U_{RF}^2}{M\Omega^2 r_0^4}, \quad (2)$$

where ϵ_0 denotes the permittivity of vacuum, U_{RF} the RF amplitude, M the trapped ion mass, $r_0 = 6.2\text{ mm}$ the radial distance from the trap axis to the electrodes, and Ω the trap driving frequency. In our experiment setup, $U_{RF} = 241\text{ V}$ and $\Omega = 2\pi \times 1.994\text{ MHz}$. The ion densities of $^{174}\text{Yb}^+$ and $^{113}\text{Cd}^+$ were thus estimated to be $7.67 \times 10^3\text{ mm}^{-3}$ and $1.18 \times 10^4\text{ mm}^{-3}$, respectively. Typical population numbers of the $^{174}\text{Yb}^+$ and $^{113}\text{Cd}^+$ ions in the two-component crystal are $N_{\text{Yb}^+} = 3.3(4) \times 10^3$ and $N_{\text{Cd}^+} = 6.9(3) \times 10^3$, which is more than that in a $^{40}\text{Ca}^+$ - $^{113}\text{Cd}^+$ sympathetic cooled crystal.

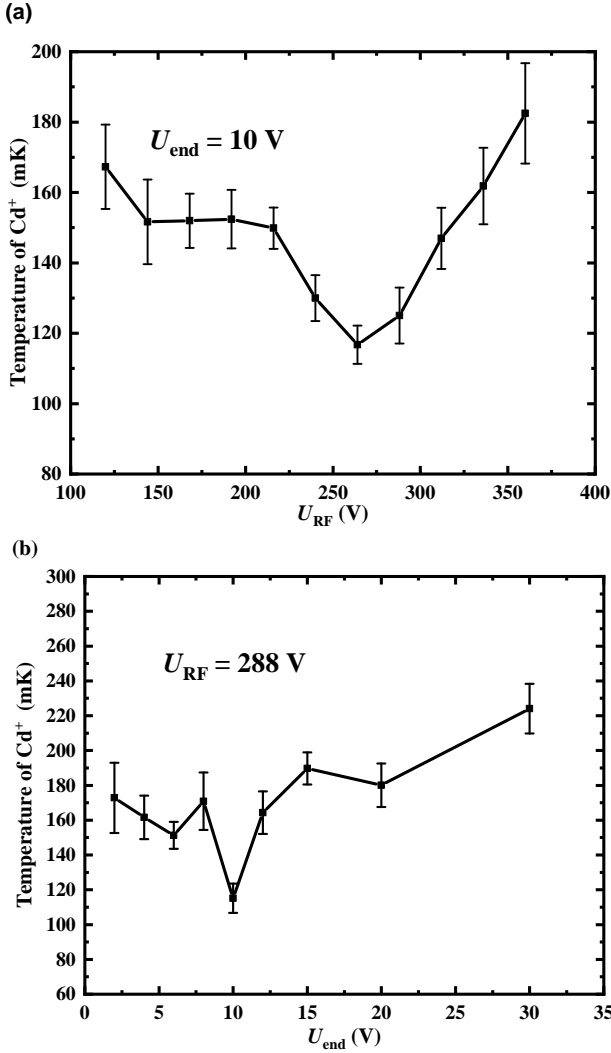


FIG. 3. Influence of electrical parameters on the temperature of sympathetically cooled $^{113}\text{Cd}^+$. (a) Temperature at different U_{RF} with $U_{\text{end}} = 10$ V. (b) Temperature at different U_{end} with $U_{\text{RF}} = 288$ V.

The SNR of microwave frequency standard depends mainly on the number of trapped ions. While $^{113}\text{Cd}^+$ ions were trapped in the outer shell of the $^{40}\text{Ca}^+ \cdot ^{113}\text{Cd}^+$ two-component Coulomb crystal, RF heating and second-order Doppler effect prevent increasing the number of ions. Trapping $^{113}\text{Cd}^+$ ions in the center avoids the problem and by increasing the number of $^{113}\text{Cd}^+$ ions we could improve the SNR of the system.

After trapping the mixed-species Coulomb crystal, the effect of RF voltage and endcap voltage (U_{end}) on the temperature of the $^{113}\text{Cd}^+$ were explored. The temperature is calculated by measuring the Doppler broadening of the fluorescence spectrum^{31,32}. Fluorescence line of ions usually follows a Voigt line, a convolution of the natural linewidth and Gaussian width of the Doppler broadening. After obtaining the Gaussian linewidth, the ion temperature is calculated using

$$T = \frac{Mc^2}{8 \ln 2 \times k_B} \left(\frac{v_G}{v_c} \right)^2, \quad (3)$$

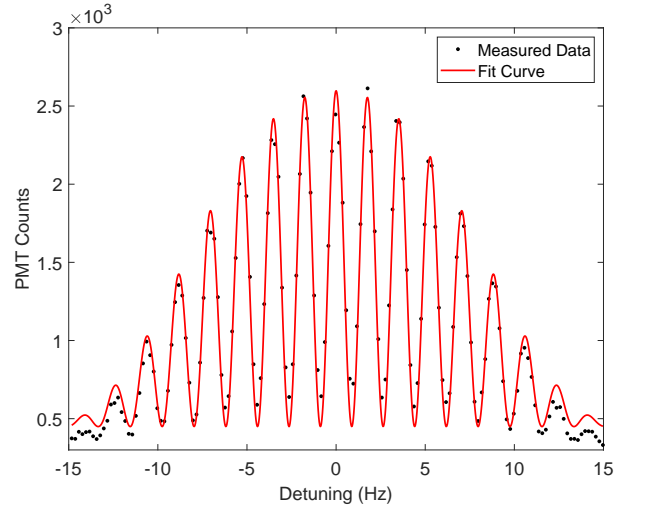


FIG. 4. Typical Ramsey fringe of the clock transition (15.2 GHz) with a free evolution time of 500 ms.

where c denotes the speed of light, k_B the Boltzmann constant, v_G the fitted Gaussian linewidth and v_c the resonance frequency of the D_2 line of $^{113}\text{Cd}^+$. Fig. 3 (a) reveals the dependence of the temperature of sympathetically-cooled $^{113}\text{Cd}^+$ on U_{RF} . As RF voltage increases, the radial size of the $^{113}\text{Cd}^+$ ion crystal is compressed, leading to less RF heating but resulting in an increase in micro-motion energy. Thus, there is an optimal value for RF voltage of approximately $U_{\text{RF}} = 264$ V. Similarly, increasing U_{end} increases the ion radial size. However, if U_{end} is too low, the ion trap becomes unstable. The optimal U_{end} is approximately 10 V as shown in Fig. 3 (b).

In this situation, a preliminary-acquired Ramsey fringe of the clock transition (Fig. 4) is obtained with a free evolution time of 500 ms. We will enhance the SNR by optimizing the electric parameters and the population number ratio to realize a sympathetically-cooled ion microwave frequency standard exhibiting high performance. The expected short-term and long-term frequency stabilities are $2 \times 10^{-13}/\sqrt{\tau}$ and 5×10^{-15} @ 10000s.

The main uncertainties of frequency shifts in the $^{174}\text{Yb}^+ \cdot ^{113}\text{Cd}^+$ sympathetic cooling system were carefully evaluated. The SOZS, which is the main source of systematic uncertainty for an ion microwave frequency standard is given by

$$\frac{\delta v_{\text{SOZFS}}}{v_0} = \frac{(g_J - g_I)^2 \mu_B^2 B^2}{2h^2 v_0^2} \quad (4)$$

where μ_B denotes Bohr magneton, B the magnetic field intensity, h Planck constant, v_0 the transition frequency of $^{113}\text{Cd}^+$ between states $|^2S_{1/2}, F=0, m_F=0\rangle$ and $|^2S_{1/2}, F=1, m_F=0\rangle$ at zero magnetic field, and for which the values for the electronic and nuclear Landé g-factors^{33,34} are $g_J = 2.002291(4)$ and $g_I = 0.6223009(9) \times 10^{-3}$, respectively. Because the $^{113}\text{Cd}^+$ ions were trapped in the center, where the magnetic gradient perpendicular to the quantization axis (e_z) is smaller, the magnetic field required to provide the quantization axis

for clock ions was reduced while measuring the clock transition signal of the $^{113}\text{Cd}^+$ ions sympathetically cooled via the $^{174}\text{Yb}^+$ ions with the magnetic fields along e_x and e_y well compensated. While collecting the Ramsey signal of the microwave clock transition, the static magnetic field is measured to be 648.1 nT, an order of magnitude smaller than before¹⁸. The fluctuation of the magnitude field under our high-performance magnetic shielding can be weakened to 0.18 nT¹⁴. Thus, SOZS is estimated to be $7.133(4) \times 10^{-13}$. Compared with the previous generation of sympathetically-cooled microwave clock, the absolute value of SOZS is reduced by more than two orders of magnitude and the uncertainty is raised by more than two orders of magnitude.

One important reason why we introduced $^{174}\text{Yb}^+$ ions as coolant is to reduce SODS. Secular motion, micro-motion and excess micro-motion through deviations from the central axis of the trap contribute to SODS. The first two contributions correlate with the secular temperature of the ions, and the last is determined by the position of the $^{113}\text{Cd}^+$ ion crystal²⁴. In the experiment, the typical temperature measurement result of sympathetically-cooled $^{113}\text{Cd}^+$ is shown in Fig. 5. The corresponding ion temperature is 100(5)mK, much smaller than that of laser-cooled $^{113}\text{Cd}^+$ (654 mK)¹⁷. The secular motion and micro-motion of the trapped ions are of the same magnitude in all directions²³. Therefore, the reduction in the axial temperature we measured is crucial for the further development of microwave ion clocks. The formula of the SODS caused contributed by excess micro-motion is²⁴:

$$\frac{\delta v_{\text{SODS-exmm}}}{\nu_0} = -\frac{1}{16} \frac{q^2 \Omega^2 u^2}{c^2} \quad (5)$$

$$q = \frac{2Q U_{\text{RF}}}{M \Omega^2 r_0^2}$$

where Q denotes the charge of $^{113}\text{Cd}^+$ and u the distance of ions from the central axis. For large ion crystals, it is in-

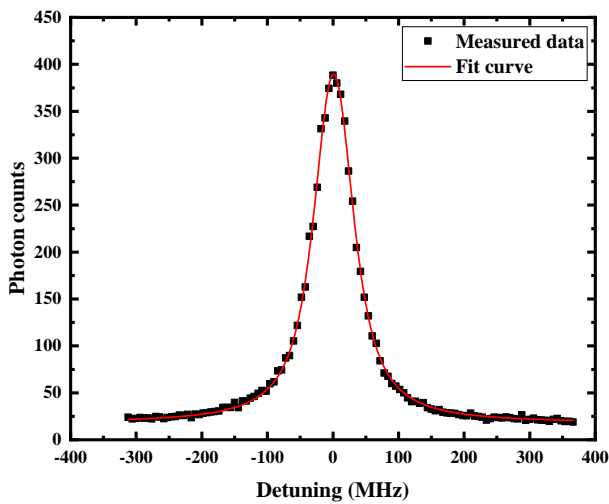


FIG. 5. Typical fluorescence line of temperature measurement of sympathetically-cooled $^{113}\text{Cd}^+$.

evitable that ions deviate from the central axis of the Paul trap.

This problem is particularly prominent when $^{113}\text{Cd}^+$ ions were cooled by $^{40}\text{Ca}^+$ ions and located in the outer shell¹⁸. Our method mitigates this effect which is why we consider $^{174}\text{Yb}^+ \text{-} ^{113}\text{Cd}^+$ sympathetic cooling suitable for microwave ion frequency standard. Calculating distances from the EMCCD images, the SODS involved with excess micro-motion is estimated to be $-7.8(5) \times 10^{-15}$, which is three times smaller than that of $^{40}\text{Ca}^+ \text{-} ^{113}\text{Cd}^+$ sympathetic cooling. Moreover, the uncertainty is six times smaller than before¹⁸. The SODS contributed by secular motion and micro-motion is calculated to be $-3.7(2) \times 10^{-16}$. Finally, the total SODS is estimated to be $-8.1(5) \times 10^{-15}$.

The Stark shift generated by the additional static electric field can be described by the following formula²³:

$$\frac{\delta v_{\text{DC-S}}}{\nu_0} = -\frac{2\sigma_S}{\nu_0} \left(\frac{m\Omega c}{Q} \right)^2 \frac{\delta v_{\text{SODS-exmm}}}{\nu_0}, \quad (6)$$

where σ_S denotes the static Stark shift coefficient. This term is proportional to the SODS produced by excess micro-motion and therefore is reduced to $7.9(5) \times 10^{-17}$.

Additional ac Stark(light) shifts introduced by the cooling(369 nm) and repumping(935nm) laser beams of $^{174}\text{Yb}^+$ were evaluated. The intensities of the 369 nm and 935 nm beams were 0.264(3) mW/mm² and 2.123(6) mW/mm², respectively, yielding the light shifts of $1.77(2) \times 10^{-17}$ and $6.21(2) \times 10^{-17}$, respectively, which can be nearly negligible for microwave frequency standard.

In conclusion, we performed a study of $^{174}\text{Yb}^+ \text{-} ^{113}\text{Cd}^+$ sympathetic cooling and proved its key advantages in a microwave ion frequency standard. Compared with laser cooling, sympathetic cooling overcomes the rising temperature of ions during interrogation, reduces the dead time, and greatly prolongs the free evolution time in closed-loop locking. Compared with using $^{40}\text{Ca}^+$ to sympathetically cool $^{113}\text{Cd}^+$, the mass difference between $^{174}\text{Yb}^+$ and $^{113}\text{Cd}^+$ is smaller, which is advantageous in promoting cooling efficiency and extending ion-loss time. Table I lists the fundamental fractional systematic uncertainties for frequency shifts among the three schemes^{17,18}. Under $^{174}\text{Yb}^+ \text{-} ^{113}\text{Cd}^+$ sympathetic cooling, the SODS uncertainty was reduced to 5×10^{-16} because excess micro-motion was substantially suppressed. The SOZS and its uncertainty were also considerably reduced to $7.133(4) \times 10^{-13}$. In addition, the introduced Stark shift from the static electric field and its uncertainty were estimated to $7.9(5) \times 10^{-17}$, which is superior by nearly an order of magnitude to our prior work¹⁸. The light frequency shift was evaluated to be $7.98(4) \times 10^{-17}$. These results show that $^{174}\text{Yb}^+ \text{-} ^{113}\text{Cd}^+$ sympathetic cooling applied to a microwave frequency standard promises to attain high accuracy of 10^{-16} and high stability.

In the future, we will study the thermodynamic properties of the $^{174}\text{Yb}^+ \text{-} ^{113}\text{Cd}^+$ ion crystal at low temperatures based on sympathetic cooling in combination with molecular dynamics simulations and experiments to elicit further advantages for the microwave frequency standard.

The $^{174}\text{Yb}^+ \text{-} ^{113}\text{Cd}^+$ crystallization results enrich the research on large two-component ion crystals, which will be meaningful for research on structures of Coulomb

TABLE I. Comparison of the fundamental fractional systematic uncertainties for frequency shifts among the laser-cooling, $^{40}\text{Ca}^+$ - $^{113}\text{Cd}^+$ sympathetic cooling and $^{174}\text{Yb}^+$ - $^{113}\text{Cd}^+$ sympathetic cooling microwave frequency standards.

Item	Laser-cooling	$^{40}\text{Ca}^+$ - $^{113}\text{Cd}^+$	$^{174}\text{Yb}^+$ - $^{113}\text{Cd}^+$
SOZS uncertainty	3×10^{-15}	1.1×10^{-14}	4×10^{-16}
SODS uncertainty	3.6×10^{-15}	3×10^{-15}	5×10^{-16}
AC Stark shift (laser)	0	$5.4(5) \times 10^{-17}$	$7.98(4) \times 10^{-17}$
Additional Stark shift	Not Mentioned	$2.3(3) \times 10^{-16}$	$7.9(5) \times 10^{-17}$

crystals^{35,36}, high-precision measurements of isotope shifts³⁷, the dynamics of an ion or small ion crystal³⁸, radioactive ions³⁹ and quantum simulations⁴⁰ based on the sympathetic cooling technique.

ACKNOWLEDGMENTS

This work is supported by National Key Research and Development Program of China (2021YFA1402100), National Natural Science Foundation of China (12073015) and the Science and Technology on Metrology and Calibration Laboratory (Grant No. JLKG2022001A002).

DATA AVAILABILITY STATEMENT

Data supporting the findings of this study are available upon reasonable request from the corresponding author.

- ¹N. Hinkley, J. A. Sherman, N. B. Phillips, M. Schioppo, N. D. Lemke, K. Beloy, M. Pizzocaro, C. W. Oates, and A. D. Ludlow, "An atomic clock with 10–18 instability," *Science* **341**, 1215–1218 (2013).
- ²V. Dzuba, V. Flambaum, M. Safronova, S. Porsev, T. Pruttivarasin, M. Hohensee, and H. Häffner, "Strongly enhanced effects of lorentz symmetry violation in entangled yb+ ions," *Nature Physics* **12**, 465–468 (2016).
- ³P. Weislo, P. Morzyński, M. Bober, A. Cygan, D. Lisak, R. Ciurylo, and M. Zawada, "Experimental constraint on dark matter detection with optical atomic clocks," *Nature Astronomy* **1**, 0009 (2016).
- ⁴M. Safronova, D. Budker, D. DeMille, D. F. J. Kimball, A. Derevianko, and C. W. Clark, "Search for new physics with atoms and molecules," *Reviews of Modern Physics* **90**, 025008 (2018).
- ⁵T. Bandi, C. Affolderbach, C. E. Calosso, and G. Mileti, "High-performance laser-pumped rubidium frequency standard for satellite navigation," *Electronics letters* **47**, 698–699 (2011).
- ⁶L. A. Mallette, J. White, and P. Rochat, "Space qualified frequency sources (clocks) for current and future gnss applications," in *IEEE/ION Position, Location and Navigation Symposium* (IEEE, 2010) pp. 903–908.
- ⁷J. D. Prestage and G. L. Weaver, "Atomic clocks and oscillators for deep-space navigation and radio science," *Proceedings of the IEEE* **95**, 2235–2247 (2007).
- ⁸E. Burt, J. Prestage, R. Tjoelker, D. Enzer, D. Kuang, D. Murphy, D. Robison, J. Seubert, R. Wang, and T. Ely, "Demonstration of a trapped-ion atomic clock in space," *Nature* **595**, 43–47 (2021).
- ⁹D. Piester, M. Rost, M. Fujieda, T. Feldmann, and A. Bauch, "Remote atomic clock synchronization via satellites and optical fibers," *Advances in Radio Science* **9**, 1–7 (2011).
- ¹⁰S. A. Diddams, J. C. Bergquist, S. R. Jefferts, and C. W. Oates, "Standards of time and frequency at the outset of the 21st century," *Science* **306**, 1318–1324 (2004).
- ¹¹E. A. Burt, W. A. Diener, and R. L. Tjoelker, "A compensated multi-pole linear ion trap mercury frequency standard for ultra-stable timekeeping,"

IEEE transactions on ultrasonics, ferroelectrics, and frequency control **55**, 2586–2595 (2008).

- ¹²B. B. Yan, H. Liu, Y. H. Chen, G. Liu, W. C. Liu, J. Wang, and L. She, "Research progress on mercury ion microwave clock for time keeping," in *China Satellite Navigation Conference (CSNC 2022) Proceedings: Volume III* (Springer, 2022) pp. 345–352.
- ¹³S. Mulholland, H. Klein, G. Barwood, S. Donnellan, D. Gentle, G. Huang, G. Walsh, P. Baird, and P. Gill, "Laser-cooled ytterbium-ion microwave frequency standard," *Applied Physics B* **125**, 198 (2019).
- ¹⁴N. C. Xin, H. R. Qin, S. N. Miao, Y. T. Chen, Y. Zheng, J. Z. Han, J. W. Zhang, and L. J. Wang, "Laser-cooled 171 yb+ microwave frequency standard with a short-term frequency instability of $8.5 \times 10^{-13}/\sqrt{\tau}$," *Optics Express* **30**, 14574–14585 (2022).
- ¹⁵J. W. Zhang, S. G. Wang, K. Miao, Z. B. Wang, and L. J. Wang, "Toward a transportable microwave frequency standard based on laser-cooled 113 cd+ ions," *Applied Physics B* **114**, 183–187 (2014).
- ¹⁶K. Miao, J. W. Zhang, X. L. Sun, S. G. Wang, A. M. Zhang, K. Liang, and L. J. Wang, "High accuracy measurement of the ground-state hyperfine splitting in a 113 cd+ microwave clock," *Optics letters* **40**, 4249–4252 (2015).
- ¹⁷S. N. Miao, J. W. Zhang, H. R. Qin, N. C. Xin, J. Z. Han, and L. J. Wang, "Precision determination of the ground-state hyperfine splitting of trapped 113 cd+ ions," *Optics letters* **46**, 5882–5885 (2021).
- ¹⁸H. R. Qin, S. N. Miao, J. Z. Han, N. C. Xin, Y. T. Chen, J. W. Zhang, L. J. Wang, *et al.*, "High-performance microwave frequency standard based on sympathetically cooled ions," *Physical Review Applied* **18**, 024023 (2022).
- ¹⁹Y. N. Zuo, J. Z. Han, L. Wei, J. W. Zhang, and L. J. Wang, "Progress towards a cadmium ion microwave clock based on sympathetic cooling," in *2018 IEEE International Frequency Control Symposium (IFCS)* (IEEE, 2018) pp. 1–3.
- ²⁰J. Z. Han, H. R. Qin, N. C. Xin, Y. M. Yu, V. Dzuba, J. W. Zhang, and L. J. Wang, "Toward a high-performance transportable microwave frequency standard based on sympathetically cooled 113cd+ ions," *Applied Physics Letters* **118**, 101103 (2021).
- ²¹Y. N. Zuo, J. Z. Han, J. W. Zhang, and L. J. Wang, "Direct temperature determination of a sympathetically cooled large 113cd+ ion crystal for a microwave clock," *Applied Physics Letters* **115**, 061103 (2019).
- ²²S. N. Miao, H. R. Qin, N. C. Xin, J. Z. Han, Y. T. Chen, J. W. Zhang, and L. J. Wang, "Sympathetic cooling of a large 113cd+ ion crystal with 40ca+ in a linear paul trap," *Chinese Journal of Physics* **83**, 242–252 (2023).
- ²³D. Berkeland, J. Miller, J. C. Bergquist, W. M. Itano, and D. J. Wineland, "Minimization of ion micromotion in a paul trap," *Journal of applied physics* **83**, 5025–5033 (1998).
- ²⁴S. N. Miao, J. W. Zhang, Y. Zheng, H. R. Qin, N. C. Xin, Y. T. Chen, J. Z. Han, and L. J. Wang, "Second-order doppler frequency shifts of trapped ions in a linear paul trap," *Physical Review A* **106**, 033121 (2022).
- ²⁵S. N. Miao, J. W. Zhang, N. C. Xin, L. M. Guo, H. X. Hu, W. X. Shi, H. R. Qin, J. Z. Han, and L. J. Wang, "Research on sympathetic cooling 113 cd+-174 yb+ system by molecular dynamics simulation," in *2021 Joint Conference of the European Frequency and Time Forum and IEEE International Frequency Control Symposium (EFTF/IFCS)* (IEEE, 2021) pp. 1–3.
- ²⁶L. Guo, *Study on Spectrum and Laser Frequency Stabilization of Yb Hollow Cathode Lamp*, Master's thesis, Tsinghua University (2021).
- ²⁷L. Hornekær, *Single-and multi-species Coulomb ion crystals: Structures, dynamics and sympathetic cooling*, Ph.D. thesis, The University of Aarhus (2000).

- ²⁸L. Hornekær, N. Kjærgaard, A. Thommesen, and M. Drewsen, “Structural properties of two-component coulomb crystals in linear paul traps,” *Physical review letters* **86**, 1994 (2001).
- ²⁹T. O’Neil, “Centrifugal separation of a multispecies pure ion plasma,” *The Physics of Fluids* **24**, 1447–1451 (1981).
- ³⁰D. Wineland, “Ion traps for large storage capacity,” in *Proceedings of the Cooling, Condensation, and Storage of Hydrogen Cluster Ions Workshop, Menlo Park* (Citeseer, 1987) p. 181.
- ³¹D. Larson, J. C. Bergquist, J. J. Bollinger, W. M. Itano, and D. J. Wineland, “Sympathetic cooling of trapped ions: A laser-cooled two-species nonneutral ion plasma,” *Physical review letters* **57**, 70 (1986).
- ³²J. Bollinger and D. Wineland, “Strongly coupled nonneutral ion plasma,” *Physical review letters* **53**, 348 (1984).
- ³³J. Z. Han, R. Si, H. R. Qin, N. C. Xin, Y. T. Chen, S. N. Miao, C. Y. Chen, J. W. Zhang, and L. J. Wang, “Determination of hyperfine splittings and Landé g factors of $5s\ 2s\ 1/2$ and $5p\ 2p\ 1/2, 3/2$ states of cd^+ 111, 113 for microwave frequency standards,” *Physical Review A* **106**, 012821 (2022).
- ³⁴P. Spence and M. McDermott, “Optical orientation of $6.7\ h107\ cd$,” *Physics Letters A* **42**, 273–274 (1972).
- ³⁵P. Richerme, “2d ion crystals in radiofrequency traps for quantum simulation,” arXiv preprint arXiv:1604.08523 (2016).
- ³⁶M. D’Onofrio, Y. Xie, A. Rasmusson, E. Wolanski, J. Cui, and P. Richerme, “Radial two-dimensional ion crystals in a linear paul trap,” *Physical Review Letters* **127**, 020503 (2021).
- ³⁷F. Gebert, Y. Wan, F. Wolf, C. N. Angstmann, J. C. Berengut, and P. O. Schmidt, “Precision isotope shift measurements in calcium ions using quantum logic detection schemes,” *Physical review letters* **115**, 053003 (2015).
- ³⁸M. Guggemos, D. Heinrich, O. Herrera-Sancho, R. Blatt, and C. Roos, “Sympathetic cooling and detection of a hot trapped ion by a cold one,” *New Journal of Physics* **17**, 103001 (2015).
- ³⁹K. Groot-Berning, F. Stopp, G. Jacob, D. Budker, R. Haas, D. Renisch, J. Runke, P. Thörle-Pospiech, C. E. Düllmann, and F. Schmidt-Kaler, “Trapping and sympathetic cooling of single thorium ions for spectroscopy,” *Physical Review A* **99**, 023420 (2019).
- ⁴⁰M. Raghunandan, F. Wolf, C. Ospelkaus, P. O. Schmidt, and H. Weimer, “Initialization of quantum simulators by sympathetic cooling,” *Science Advances* **6**, eaaw9268 (2020).